

Competition between SFG and two SHGs in broadband type-I QPM

Weirui Dang · Yuping Chen · Mingjun Gong · Xianfeng Chen

Received: 29 June 2012 / Accepted: 14 September 2012 / Published online: 16 January 2013
© Springer-Verlag Berlin Heidelberg 2013

Abstract In this paper, we have studied the characteristics of second-order nonlinear interactions with band-overlapped type-I quasi-phase-matching (QPM) second harmonic generation (SHG) and sum-frequency generation (SFG), and predicted a blue-shift with a band-narrowing of their bands and a sunken response in the SFG curve, which are due to the phase-matching-dependent competition between band-overlapped SHG and SFG processes. This prediction is then verified by the experiment in an 18-mm-long bulk MgO-doped periodically poled lithium niobate crystal (MgO:PPLN) and may provide the candidate solution to output controlling for flexible broadcast wavelength conversion, channel-selective wavelength conversion and all-optical logic gates by cascaded QPM second-order nonlinear processes.

1 Introduction

In future all-optical networks, wavelength conversion is a crucial function to be required in signal path routing and wavelength division multiplexing (WDM), which will enable the effective usage of the vast fiber bandwidth and flexible network construction [1]. Among various approaches of all-optical wavelength conversion schemes, the cascaded sum- and difference-frequency generation (cSFG/DFG) [2–6], and cascaded second harmonic and

difference-frequency generation (cSHG/DFG) [7–11] in a periodically poled lithium niobate (PPLN) is the most promising: in addition to strict transparency and independence of bit rate and data format, it has negligible spontaneous emission noise and has no intrinsic frequency chirp [12]. In 2002, Nan Ei Yu et al. reported experimentally a broadband second harmonic generation (SHG) at the communication band using type-I quasi-phase-matching (QPM) in PPLN [13]. Based on this type-I QPM, flexible wavelength conversion and $N \times M$ wavelength broadcast [11, 14] have been realized by cSHG/DFG. As a result, the first nonlinear process in cascading interaction—broadband QPM SHG or sum-frequency generation (SFG) provides a flexible and controllable scheme to realize flexible wavelength conversion. In this paper, we investigate the dependences of second harmonic (SH) and sum-frequency (SF) waves with the broadband QPM second-order nonlinear phase-matching condition in MgO-doped PPLN (MgO:PPLN) in detail. In a bulk MgO:PPLN, we predict and then experimentally verify the competition between SFG and SHG within this broad sum-frequency band. The band-overlapped second-order nonlinear interactions of SFG and SHG can be employed as multi-broadcast wavelength conversion by cascading DFG.

2 Characteristics of second-order nonlinear interactions and type-I QPM SHG and SFG experiments

To realize the efficient QPM SHG and SFG, the wavelengths of two pump lights, λ_{P1} and λ_{P2} , need to satisfy the following type-I QPM conditions perfectly:

$$\begin{aligned} 2\pi n_{SF}/\lambda_{SF} - 2\pi n_{P1}/\lambda_{P1} - 2\pi n_{P2}/\lambda_{P2} &= 2\pi/\Lambda, \\ 1/\lambda_{SF} &= 1/\lambda_{P1} + 1/\lambda_{P2} \end{aligned} \quad (1)$$

W. Dang · Y. Chen (✉) · M. Gong · X. Chen
Department of Physics, The State Key Laboratory on Fiber Optics Local Area Communication Networks and Advanced Optical Communication Systems, Shanghai Jiao Tong University, 200240 Shanghai, China
e-mail: ypchen@sjtu.edu.cn

X. Chen
e-mail: xfchen@sjtu.edu.cn

where Λ is the period of the periodical domain inverted structure; n_i ($i = P1, P2, SF$) is the refractive index at the pump and SFG wavelengths, respectively. Due to the low dispersion around 1,550 nm in MgO-doped LiNbO₃ crystals [3], it can be proved that the QPM conditions shown in Eq. (1) for SFG process will be almost entirely satisfied if the two pumps are located around 1,550 nm. So is the SHG process. Figure 1 shows the theoretical bandwidths of type-I QPM SFG and SHG at 38.0 °C, respectively, which are calculated by Sellmeier equations [15] of 5 mol % MgO:PPLN with a grating period of 20.4 μm . The dashed line stands for the SHG band of pump light, while the solid line is the behavior of SFG band with pump2 wavelength fixed at 1,572 nm and pump1 wavelength turning from 1,520 to 1,600 nm. The two curves are calculated respectively, and the theoretical bandwidths are observed to be 25 and 44 nm, respectively. Here, we notice that the SHG band is covered by the SFG band, which means the two second-order nonlinear processes interact with each other since they both consume energy from given pumps. So in the next part of this article, we investigate experimentally how this “interaction” evolves and how the two processes compete with each other, which may provide detailed useful data and solution to how to control the output conversion wavelength for the flexible wavelength conversion by cascading QPM second-order nonlinear processes.

Figure 2 shows the experimental setup for broadband type-I QPM SHG and SFG. In this scheme, two tunable lasers at wavelengths λ_{P1} and λ_{P2} serve as two pump sources, which are used to generate the short-wavelength light required in the following SHG and SFG processes. The two pump lights are mixed by a coupler and then amplified by an erbium-doped fiber amplifier (EDFA). A collimator and a lens are utilized to adjust the amplified lights to uniform beams which inject into the bulk 5 mol % MgO:PPLN. The output spectra are monitored by an

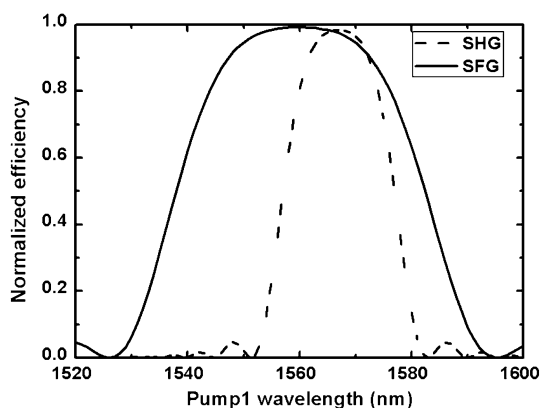


Fig. 1 Calculated broadband type-I QPM SFG and SHG

optical spectrum analyzer (OSA). The size of the z-cut MgO:PPLN crystal is $18 \times 10 \times 0.5$ mm, and its grating period is 20.4 μm . Temperature of the crystal is controlled by a temperature controller (TC) with an accuracy of 0.1 °C. Two polarization controllers (PC) are employed to adjust the polarization of pump lights at the ordinary direction which guarantees the type-I QPM in this crystal.

In our experiment, the operation temperature of the MgO:PPLN crystal is set at the optimum temperature 38.0 °C. The pump2 wavelength is fixed at 1,572 nm while pump1 wavelength varies. The input powers of the two pumps are equal. Three different observations of second-order nonlinear interactions are shown in Fig. 3. It is worth noticing that the SF wave always exists, while the SH waves appear alternatively depending on the pump1 wavelength tuning. From Fig. 3b, we can see clearly that the SHG intensities arise to almost half of the SFG intensity as pump1 wavelength is located at 1,542 nm. When pump1 wavelength turns to 1,534 nm in Fig. 3a, only SHG2 and SFG appear with comparable intensities. In Fig. 3c, pump1 wavelength turns to 1,558 nm, so both SHG1 and SFG dominate while SHG2 almost disappears.

According to the QPM theory [16], we believe that the relative intensity changes between SFG and SHGs depend on which process is more close to the perfect QPM conditions. In other words, the competition between SFG and SHG 1 and 2 depends on the phase mismatching ($|\Delta k|$) condition, which is shown in Fig. 3d. Since the vertical dashed lines represent 1,534, 1,542, and 1,558 nm, respectively, the points they intersect with each curves represent the phase mismatching of SFG, SHG1, and SHG2 when pump1 is tuned at corresponding wavelength. At 1,534 nm, we can see that the phase mismatch of SH1 (medial red circle) is much smaller than that of SH2 (upper red circle), but is comparable with that of SFG (lower red circle). Hence SH2 and SFG intensities are relatively large in Fig. 3a while SH1 almost disappears. When pump1 moves to 1,542 nm, the phase mismatch of SH1 (medial blue circle) and SH2 (upper blue circle) are both small but the phase mismatch of SFG (lower blue circle) is almost zero. That is why both SH1 and SH2 intensities in Fig. 3b



Fig. 2 Type-I QPM SHG and SFG experimental setup

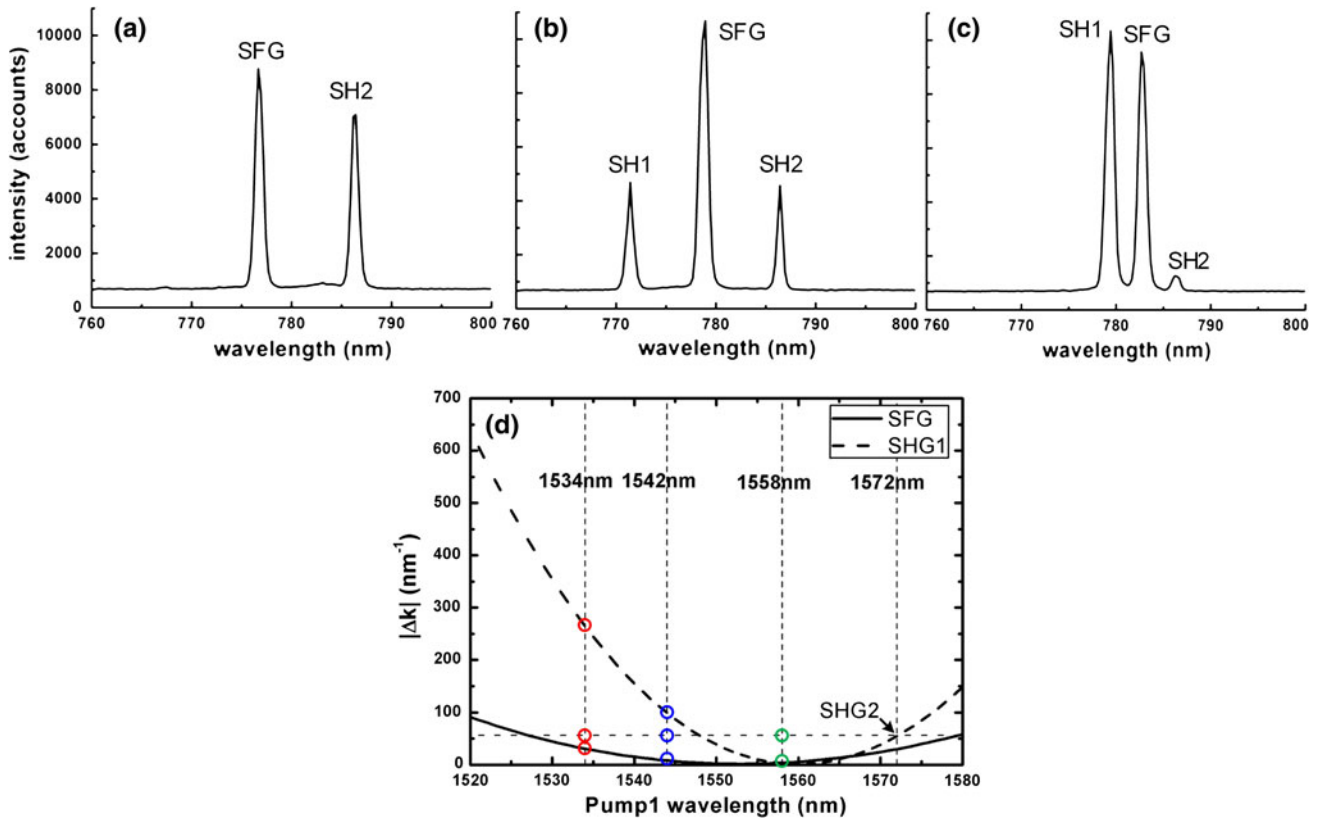


Fig. 3 Band-overlapped SFG and SHGs, $\lambda_{p2} = 1,572$ nm, λ_{p1} is at **a** 1,534 nm; **b** 1,542 nm; **c** 1,558 nm, and **d** the phase mismatch of SFG and SHGs along with tuned pump1 and fixed pump2 waves. In **d**,

red, blue and green circles correspond to the phase mismatch conditions of SFG (solid line), SHG1 (dashed line) and SHG2 in accordance with the competition results in **a**, **b**, and **c**, respectively

are lower than SFG intensity. Figure 3c accords with green circles in Fig. 3d, where pump1 wavelength is located at 1,558 nm. The phase mismatch of SH1 and SFG are both around zero (lower green circle) while the phase mismatch of SH2 (upper green circle) seems to be much bigger, which leads to a small SH2 intensity and large SFG and SH1 intensities in Fig. 3c. This accordance between the measured intensities and calculated phase mismatching conditions suggests that the competition between SFG and SHG is highly phase-mismatching-dependent.

3 Numerically theoretical and experimental results and analysis

To study the competition process more clearly, we carry out the numerical simulations of band-overlapped SHG and SFG in MgO:PPLN crystal. These broadband type-I QPM second-order nonlinear processes can be described under the slowly varying amplitude and small signal approximations by five coupled wave equations as follows [16]:

$$dA_{P1}/dx = -i\kappa_{SH1}A_{P1}^*A_{SH1}e^{-i\Delta k_{SH1}x}/2 - i\kappa_{SF}A_{P2}^*A_{SF}e^{-i\Delta k_{SF}x}, \tag{2}$$

$$dA_{P2}/dx = -i\kappa_{SH2}A_{P2}^*A_{SH2}e^{-i\Delta k_{SH2}x}/2 - i\kappa_{SF}A_{P1}^*A_{SF}e^{-i\Delta k_{SF}x}, \tag{3}$$

$$dA_{SH1}/dx = -i\kappa_{SH1}A_{P1}^2e^{i\Delta k_{SH1}x}/2, \tag{4}$$

$$dA_{SH2}/dx = -i\kappa_{SH2}A_{P2}^2e^{i\Delta k_{SH2}x}/2, \tag{5}$$

$$dA_{SF}/dx = -i\kappa_{SF}A_{P1}A_{P2}e^{i\Delta k_{SF}x}. \tag{6}$$

Here A_i ($i = P1, P2, SH1, SH2, SF$) is amplitude and x is propagation distance. Since we use type-I QPM, Δk_i ($i = SH1, SH2, SF$) is the phase mismatching of SHG and SFG processes, respectively. The phase mismatching can be written as (Λ is the grating period of MgO:PPLN, n is refractive index):

$$\Delta k_{SH1} = 2\pi n_{2\omega_1}^e/\lambda_{SH1} - 4\pi n_{\omega_1}^o/\lambda_{P1} - 2\pi/\Lambda, \tag{7}$$

$$\Delta k_{SH2} = 2\pi n_{2\omega_2}^e/\lambda_{SH2} - 4\pi n_{\omega_2}^o/\lambda_{P2} - 2\pi/\Lambda, \tag{8}$$

$$\Delta k_{SF} = 2\pi n_{SF}^e / \lambda_{SF} - 2\pi n_{\omega_1}^o / \lambda_{P1} - 2\pi n_{\omega_2}^o / \lambda_{P2} - 2\pi / \Lambda. \quad (9)$$

κ_i ($i = \text{SH1, SH2, SF}$) is the coupled coefficient and can be defined as:

$$\begin{aligned} \kappa_{\text{SH1}} &= \frac{2d_{31}}{\pi c} \sqrt{\frac{k_{P1}^2 k_{\text{SH1}}}{n_{P1}^2 n_{\text{SH1}}^e}}, \quad \kappa_{\text{SH2}} = \frac{2d_{31}}{\pi c} \sqrt{\frac{k_{P2}^2 k_{\text{SH2}}}{n_{P2}^2 n_{\text{SH2}}^e}}, \quad \kappa_{\text{SF}} \\ &= \frac{2d_{31}}{\pi c} \sqrt{\frac{k_{P1} k_{P2} k_{\text{SF}}}{n_{P1}^o n_{P2}^o n_{\text{SF}}^e}} \end{aligned} \quad (10)$$

where the MgO:PPLN crystal length is 18 mm, pump2 wavelength is fixed at 1,572 nm, pump1 wavelength varies from 1,520 to 1580 nm, and the intensities of two input pumps are both normalized to 1 which are approximately consistent with the experimental conditions. So numerically we plot the variation curves of SHG and SFG intensities versus pump1 wavelength as shown in Fig. 4a, where the EDFA intrinsic spectrum is taken into account as the magnification band of EDFA ranges from 1,530 to 1,572 nm. The color zones represent distinctive competition relationships under this magnification band. The yellow zone denotes that the SFG process dominates and SH1 is suppressed while SH2 intensity is relative large. In the blue zone, the same case occurs except for the roles of SH1 and SH2 exchanged. A lower response in the SFG curve locates in the red zone where its intensity is smaller than the SH1 intensity while SH2 wave is suppressed.

Thus, different from aforesaid theoretical results in Fig. 1, we find the competition between band-overlapped SFG and SHG makes both the SFG band and the SHG band suffer a blue shift of 26 nm and a band-narrowing. The full width at half maximum (FWHM) of SFG band narrows from 44 to 23 nm and the FWHN of SHG band narrows from 25 to 13 nm. The theoretical conversion efficiency of SF and SH1 waves appears to be slightly lower than that in

Fig. 1, and SH2 wave is extremely suppressed while SH1 wave is relatively high. According to the QPM theory [16], we believe these changes in the second-order nonlinear optical response are ascribed to the competition between SFG and SHG process. As shown in Fig. 3d, lower phase-mismatch of SHG leads to higher intensity of SH wave, and it is the same in the case of SFG. Since the power of the pumps is finite, the two second-order nonlinear processes of SHG and SFG have to compete for energy as they are nearing the phase-matching condition. In Fig. 4a, pump2 is fixed at 1,572 nm, so the quantity of SHG2's phase mismatch is also fixed. When pump1 locates in the yellow zone, SHG1 is highly phase-mismatched, and consequently the intensity of SH1 wave is small; in comparison, SFG is lower phase-mismatched, so higher intensity of SF wave appears in the response curve. Since both the SFG and SHG1 do not consume much power of the pumps, SHG2 gets more, showing a relative importance. When pump1 locates at the blue zone, SHG1 shows a lower phase-mismatch than SHG2, leading to higher intensity of SH1 than SH2; and since the phase mismatch of SFG is lowest among them SF wave is of highest intensity. When pump1 locates in the red zone, SH2 wave is the smallest one as SHG2's phase-mismatch is highest; SHG1 consumes more power of pump1 than SFG due to its lower phase-mismatch, and with a lower response of SF wave, a consequent higher response of SH1 wave gives rise to a basin in the SF response curve and leads to a shift of SFG's band center. The competition between SFG and SHGs is notable as they are nearing the phase-matching condition, and it changes the nonlinear optical response.

To verify our prediction and give the analysis of the competition process, we measured the SFG and SHG intensities' variation which is shown in Fig. 4b, where the pump2 wavelength is fixed at 1,572 nm and pump1 wavelength is tuned from 1,530 to 1,580 nm. The

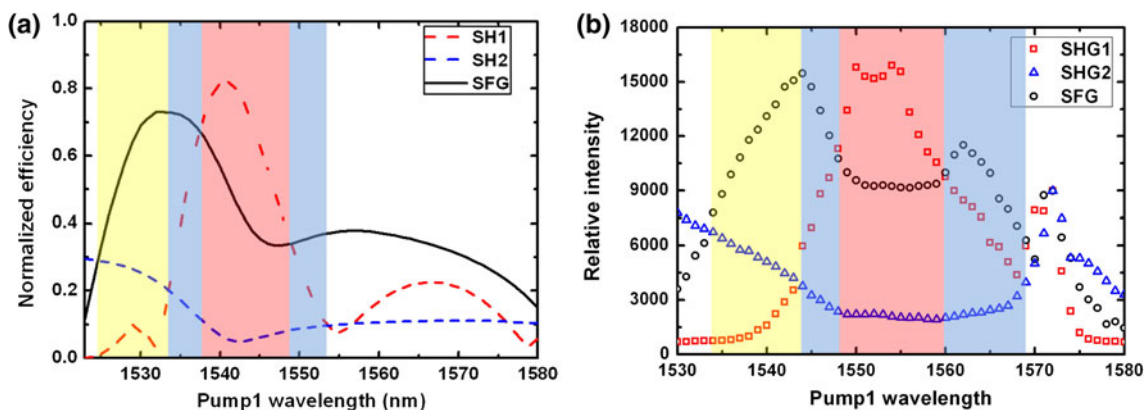


Fig. 4 **a** The calculated intensity changes of SHG1, SHG2, and SFG due to competitions, considering the influence of the EDFA intrinsic spectrum; **b** measured broadband type-I QPM SFG (black), band-

overlapped type-I QPM SHG1 and SHG2 (red for tunable pump1 wave and blue for fixed pump2 wave)

intensities of measured SFG wave, SH1 and SH2 waves are indicated by black circles, red squares and blue triangles, respectively. These three wave intensities and their competition relationships, denoted by different color zones, are both in good accordance with our theoretical prediction in Fig. 4a. The SHG band and the SFG band are found blue shifted and narrowed compared with those in Fig. 1, and a lower response in the SFG curve also appears in the red zone. Here, one difference is noticed between numerical and experiment results that in Fig. 4b, there is a drop in the SH1 curve in the red zone while it is a peak at the same wavelength range in Fig. 4a. In the numerical simulation, only two second-order nonlinear processes—SHG and SFG are mainly considered, for other nonlinear processes such as difference-frequency generation, type-0 phase-mismatched processes and high-order harmonic generations are believed to have little influence on the results. However in the experiment, except up-conversion processes (SHG and SFG), down-conversion processes may exist, for example, SH1 may be partly back-converted to the fundamental wave (pump1) due to type-0 high-order harmonic generation, and a consequent drop in the SH1 curve appears. Other difference between Fig. 4a and Fig. 4b is due to the disagreement of Sellmeier equations between that we used in numerical simulations and the actual one of the crystal in the experiment. Other differences may be attributed to non-uniform periodicity of QPM grating and operation temperature fluctuation.

4 Discussion

In summary, we investigate the phase-mismatch-dependent competition between SFG and SHG waves in MgO:PPLN crystal. This competition makes both SFG band and SHG band blue shifted when compared with the theoretical results in Fig. 1, and brings a sunken response in the SFG curve, and narrows the type-I QPM bandwidth from 44 to 35 nm for SFG and from 25 to 18 nm for SHG, which is in good accordance with our numerical prediction. This band-overlapped appearance and the competition between SFG and SHG have practical applications in all-optical wavelength conversions, since by employing two pumps, we can not only broadcast one signal to three channels, but also realize the channel-selective wavelength conversion. Furthermore, by employing N pumps in the broad tuning band, theoretically we can broadcast one signal to C_N^2 (combination number of N pumps) channels and choose the output channels by controlling their competition [2]. In addition, the competition between SFG and SHG can also be utilized to build all-optical logic controlled-NOT, XOR, and XNOR gates [17].

Acknowledgments This work is supported by the National Natural Science Fund of China (10874120 and 11174204), and sponsored by the Scientific Research Foundation for the Returned Overseas Chinese Scholars, State Education Ministry.

References

1. S.J.B. Yoo, Wavelength conversion technologies for WDM network applications. *IEEE J. Lightwave Technol.* **14**, 955 (1996)
2. C.Q. Xu, B. Chen, Cascaded wavelength conversions based on sum-frequency generation and difference-frequency generation. *Opt. Lett.* **3**, 292–294 (2004)
3. Bo Chen, Xu Chang-Qing, Analysis of novel cascaded $\chi^{(2)}$ (SFG + DFG) wavelength conversions in quasi-phase-matched waveguides. *IEEE J. Quantum Electron* **40**(3), 256–261 (2004)
4. Y.L. Lee, B.-A. Yu, C. Jung, Y.C. Noh, J. Lee, D.K. Ko, All-optical wavelength conversion and tuning by the cascaded sum- and difference frequency generation (cSFG/DFG) in a temperature gradient controlled Ti:PPLN channel waveguide. *Opt. Express* **13**, 2988–2993 (2005)
5. Y. Wang, C.Q. Xu, Analysis of picosecond-pulse wavelength conversion based on cascaded sum-frequency generation and difference-frequency generation in quasi-phase-matched LiNbO₃ waveguides. *Opt. Eng.* **46**, 055003 (2007)
6. H. Furukawa, A. Nirmalathas, N. Wada, S. Shinada, H. Tsuboya, T. Miyazaki, Tunable all-optical wavelength conversion of 160-Gb/s RZ optical signals by cascaded SFG-DFG generation in PPLN waveguide. *IEEE Photonics Technol. Lett.* **19**, 384–386 (2007)
7. M.H. Chou, I. Brener, M.M. Fejer, E.E. Chaban, S.B. Christman, 1.55- μ m-band wavelength conversion based on cascaded second-order nonlinearity in LiNbO₃ waveguides. *IEEE Photonics Technol. Lett.* **11**, 653–655 (1999)
8. O. Tadanaga, M. Asobe, H. Miyazawa, Y. Nishida, H. Suzuki, Efficient 1.55 μ m-band quasi-phase-matched ZnO-doped LiNbO₃ wavelength converter with high damage resistance. *Electron Lett.* **39**, 1525–1527 (2003)
9. J. Fonseca-Campos, Y. Wang, B. Chen, C.Q. Xu, S. Yang, E.A. Ponomarev, X. Bao, 40-GHz picosecond-pulse second-harmonic generation in an MgO-doped PPLN waveguide. *J. Lightwave Technol.* **24**, 3698–3708 (2006)
10. Y. Wang, J. Fonseca-Campos, C. Xu, S. Yang, E.A. Ponomarev, X. Bao, Picosecond-pulse wavelength conversion based on cascaded second-harmonic generation-difference frequency generation in a periodically poled lithium niobate waveguide. *Appl. Opt.* **45**, 5391 (2006)
11. J. Zhang, Y. Chen, F. Lu, X. Chen, Flexible wavelength conversion via cascaded second order nonlinearity using broadband SHG in MgO-doped PPLN. *Opt. Express* **16**(10), 6957–6962 (2008)
12. C. Langrock, S. Kumar, J.E. McGeehan, A.E. Willner, M.M. Fejer, All-optical signal processing using $\chi^{(2)}$ nonlinearities in guided-wave devices. *J. Lightwave Technol.* **24**(7), 2579–2592 (2006)
13. Nan Ei Yu, Jung Hoon Ro, Myoungsik Cha, Sunao Kurimura, Takunori Taira, Broadband quasi-phase-matched second-harmonic generation in MgO-doped periodically poled LiNbO₃ at the communications band. *Opt. Lett.* **27**(12), 1046–1048 (2002)
14. Mingjun Gong, Yuping Chen, Feng Lu, Xianfeng Chen, All optical wavelength broadcast based on simultaneous type I QPM broadband SFG and SHG in MgO:PPLN. *Opt. Lett.* **35**(16), 2672–2674 (2010)

15. D.E. Zelmon, D.L. Small, Infrared corrected Sellmeier coefficients for congruently grown lithium niobate and 5 mol % magnesium oxide-doped lithium niobate. *J. Opt. Soc. Am. B* **14**(12), 3319–3322 (1997)
16. R.W. Boyd, *Nonlinear Optics* (Academic, 1992)
17. Y.X. Zhang, Y.P. Chen, X.F. Chen, Polarization-based all-optical logic controlled-NOT, XOR, and XNOR gates employing electro-optic effect in periodically poled lithium niobate. *Appl. Phys. Lett.* **99**(16), 161117 (2011)